Mechanism of enhanced broadening of the ionization level of Li outside transition metal surfaces

Keith Niedfeldt,[1] Peter Nordlander,[2] and Emily A. Carter[1]
[1]*Department of Mechanical and Aerospace Engineering and Program in Applied and Computational Mathematics, Princeton University, Princeton, New Jersey 08544-5263, USA*
[2]*Department of Physics and Astronomy, M.S. 61, Rice University, P.O. Box 1892, 6100 South Main Street, Houston, Texas 77251-1892, USA*
(Received 30 May 2006; published 15 September 2006)

We show that the *d*-band of a transition metal surface induces intra-atomic hybridization of an atom in its vicinity. It is demonstrated that such hybridization can have a profound influence on the resonance width and hence lifetime of the atomic ionization level. The degree of Li *s*-*p* hybridization is found to be directly correlated to the overlap of the *d*-band density of states with the Li 2*s* and 2*p* levels, and is shown to be not due solely to long-range electrostatic image potential effects.

DOI: 10.1103/PhysRevB.74.115109 PACS number(s): 34.50.Dy, 31.15.Ew, 34.70.+e

Charge transfer reactions between gas phase atoms and metallic surfaces are of fundamental importance in many dynamical processes such as heterogeneous catalysis,[1,2] corrosion,[3,4] stimulated desorption,[5] and ion-surface scattering.[1,6,7] The most important fundamental physical property determining the charge transfer rate between an atom and a surface is the electron tunneling rate through the potential barrier between the atom and the surface. Electron tunneling results in a broadening of the atomic levels, i.e., the atomic levels become resonances. The resonance width is directly proportional to the electron tunneling rate. Despite their ubiquity and importance, first-principles theoretical investigations of the broadening of atomic levels near metallic surfaces have been relatively scarce.[6,8,9]

Conventional methods[10–12] for calculating the widths of atomic levels near metallic surfaces are based on one-electron approaches where simple model potentials are introduced to describe the potential energy of an electron in the surface region. The surface potential is constructed by adding an imagelike potential representing the electron-surface interaction and a pseudopotential describing the interaction of the electron with the atom. As a result, it is not possible to examine either the effect of realistic surface electronic structure or the changes of the electronic structure of the surface that result from the chemical interaction of the atom with the surface.

In a recent publication,[9] we developed a periodic density functional theory (DFT)-based deconvolution scheme to extract adsorbate energy level widths near surfaces, and applied it to an adsorbate outside a nearly free-electron-like metal surface (Al). By comparing our calculated widths with results from simpler models that neglect changes in electronic structure caused by the interaction between the surface and the adsorbate, we established that the chemical interactions between the atom and the surface can have a strong influence on the broadening of atomic levels.

In this paper, we generalize our first-principles approach and investigate the broadening of atomic levels near transition metal surfaces. We show that the chemical effects caused by the interaction between an atom and a transition metal surface can be much larger than for an atom near a nearly free-electron-like surface. In particular, we provide evidence that the *d*-band can mediate a strong mixing of the atomic levels. As was established previously for hydrogen interacting with simple metal surfaces,[10] the mixture of higher excited atomic states can significantly increase the tunneling rates between an atom and a surface. Here we demonstrate that the degree of intra-atomic hybridization correlates strongly with the magnitude of the *d*-band density of the states at the energies of the atomic levels.

Details on our scheme for calculating level widths can be found in Ref. 9. The width of the atomic resonance is calculated from the projected density of states (PDOS),[8,9,13]

$$\Pi_l(\varepsilon) = 2\pi \sum_m |\langle \phi_m | \phi_l \rangle|^2 \delta(\varepsilon - \varepsilon_m). \quad (1)$$

In Eq. (1), the PDOS $[\Pi_l(\varepsilon)]$ is a function of the energy ε and the state l onto which we are projecting. This function is evaluated by calculating the overlap of m interacting Kohn-Sham orbitals ϕ_m with the isolated atomic orbital ϕ_l. The Dirac delta function $\delta(\varepsilon - \varepsilon_m)$, where ε_m is the energy of orbital m, is then broadened using a small parameter. The PDOS so obtained is a Lorentzian from which a width can be extracted by deconvolution.[8] In our earlier application to Li scattering off Al(001), the calculated widths were in excellent agreement with experimental data.[9]

In the present application, the self-consistent valence electronic structure of Li outside a variety of main group and transition metal surfaces is calculated using the periodic DFT program CASTEP_3.2.[14] We employ the local density approximation (LDA) for the electron exchange-correlation functional, which is based upon the homogeneous electron gas quantum Monte Carlo results of Ceperley and Alder, as parametrized by Perdew and Zunger.[15,16] We find that the energy level widths are insensitive (to within <1 meV) to the choice of exchange-correlation potential, as evidenced by tests comparing energy level widths for Li/Ir(001) obtained from LDA to those from a generalized gradient approximation (GGA) to the exchange-correlation functional due to

TABLE I. Plane-wave basis kinetic energy cutoff and k-point meshes used for the given supercell models of metal surfaces studied in this work.

Supercell	Kinetic energy cutoff (eV)	k-point mesh	k-point spacing (1/a.u.)
Al(001)-$c(2\times2)$	500	$8\times8\times1$	0.030
Mg(0001)-(3×3)	400	$4\times4\times1$	0.057
Cu(001)-$c(2\times2)$	850	$4\times4\times1$	0.065
Ir(001)-$c(2\times2)$	640	$4\times4\times1$	0.062
Rh(001)-$c(2\times2)$	310	$4\times4\times1$	0.062
Ag(001)-$c(2\times2)$	340	$4\times4\times1$	0.061
Pt(001)-$c(2\times2)$	280	$4\times4\times1$	0.060
Au(001)-$c(2\times2)$	360	$4\times4\times1$	0.058

Perdew-Burke-Ernzerhof (PBE).[17] We therefore used the LDA for all other studies in this work. Norm-conserving pseudopotentials (NCPs) for Al, Mg, Cu, and Ir are taken from the Trouiller-Martins libraries created by Allan and Teter[18,19] distributed with CASTEP_4.2.[18] A more approximate PDOS method[20] is used to survey additional transition metals (Rh, Ag, Pt, and Au) using the default ultrasoft pseudopotentials (USPPs) (Ref. 21) included with CASTEP_3.2.[12] Use of supercell sizes, kinetic energy cutoffs for the plane-wave basis, and k-point meshes given in Table I converge the Li energy level widths to within 0.05 eV. As established earlier,[9] the size of supercells we employ ensures that periodic images of the Li atom are sufficiently distant that the Li energy level widths are unaffected by these images. In order to exploit mirror symmetry, a Li atom is placed on each side of the metal slab. Then, in order to avoid spurious contact (due to the periodic boundary conditions) between the two Li atoms at large Li-surface separations, periodic images of the surfaces are separated by 49 a.u. of vacuum. Seven layers of substrate metal atoms are necessary (and hence are used) to properly mimic the crystalline surface and to ensure no interaction between the Li atoms on each side of the slab.[9] Equilibrium bulk structures as predicted by DFT-LDA are employed for calculations using NCPs, while experimental bulk structures are used in the survey done with USPPs.

When a transition metal surface d-band lies close in energy to the Li $2s$ and $2p$ energy levels, we find strong polarization of the Li atom valence states as Li approaches the surface. As a result, the wave function corresponding to the ionization level of Li becomes s-p hybridized,

$$\phi_{\mathrm{Li}\ Hyb} = c_{2s}\phi_{\mathrm{Li}\ 2s} + c_{2p}\phi_{\mathrm{Li}\ 2p}. \tag{2}$$

Evidence for this transition metal surface-induced hybridization is the appearance of a second (smaller) Lorentzian peak in the PDOS obtained from Eq. (1). As an example, Fig. 1 displays PDOSs for the $2s$ and $2p$ states of Li at a distance of 10 a.u. from an Ir(001) surface. The second Lorentzian present in the Li $2s$ PDOS corresponds directly to the Lorentzian in the Li $2p$ PDOS, and vice versa. This result suggests that mixing between the Li $2s$ and $2p$ states is occurring in the presence of a transition metal surface.

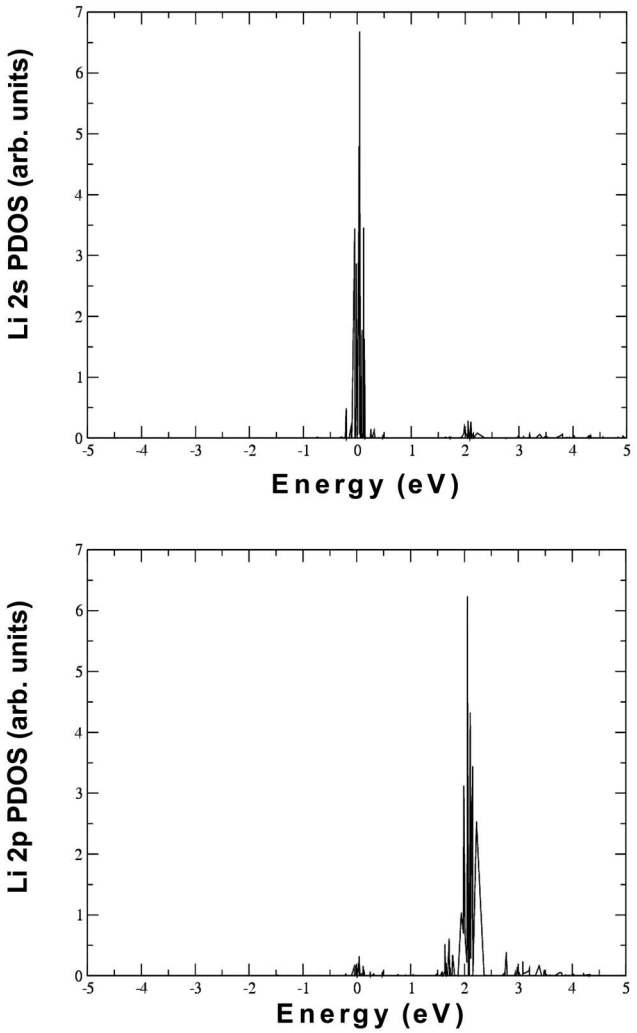

FIG. 1. PDOS for Li $2s$ (top) and Li $2p$ (bottom) for a Li atom 10 a.u. above a top site on the Ir(001) surface. 0 eV and 2.1 eV correspond to the $2s$ and $2p$ energy levels, respectively, of an isolated Li atom. Li s-p mixing is observed.

The mixing of Li $2s$ and $2p$ orbitals due to surface-induced symmetry breaking should be accounted for when calculating the effective width of the ionization level of Li. Since the level now contains a mixture of both the Li $2s$ and $2p$ levels, the width can be written as

$$\Gamma(\mathrm{Li}_{Hyb}) = \lambda_{2s}\Gamma(\mathrm{Li}_{2s}) + \lambda_{2p}\Gamma(\mathrm{Li}_{2p}). \tag{3}$$

If interference effects between the Li $2s$ and $2p$ states are neglected (their importance is assessed below), λ_{2s} and λ_{2p} simply would be the squares of the amplitudes c_{2s} and c_{2p} in Eq. (2), respectively. As we illustrate below, the magnitudes of the coefficients λ_{2s} and λ_{2p} depend strongly on atom-surface separation and the nature of the surface, and lead to widths that are very different from those obtained by neglecting Li $2p$ mixing ($\lambda_{2s}=1$ and $\lambda_{2p}=0$).

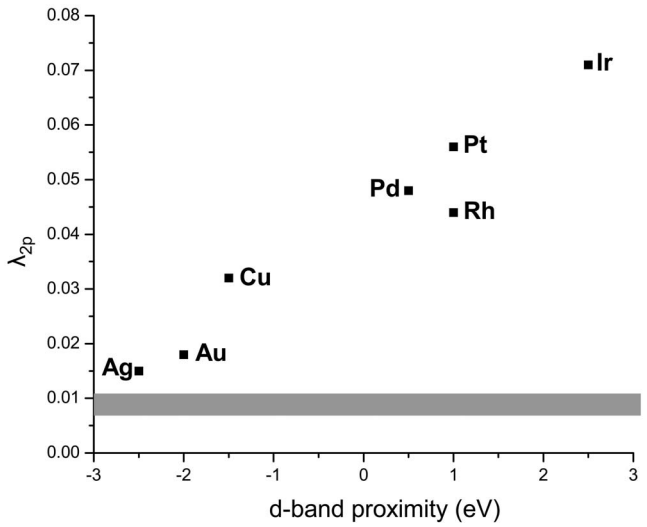

FIG. 2. Fraction of Li $2p$ PDOS [λ_{2p} in Eq. (3)] as a function of d-band proximity to the isolated Li $2s$ level. λ_{2p} is calculated for Li 10 a.u. from each metal surface. Open d-shell transition metals exhibit the largest mixing of the Li energy level widths. The horizontal shaded area corresponds to the range of λ_{2p} predicted from a jellium model that includes the image potential.

While our analysis follows the usual convention of working in the diabatic representation of pure Li $2s$ and $2p$ states, we decided to quantify the extent to which interference effects may change the quantitative widths calculated. This is accomplished by carrying out the projection of the DOS onto an adiabatic basis comprised of a linear combination of the isolated Li $2s$ and $2p$ atomic orbitals. The coefficients of these atomic orbitals were chosen such that the PDOS only display a single Lorentzian peak.[22] The width of this resonance corresponds to the inverse lifetime of the hybridized Li ionization level. The transformation to an adiabatic basis systematically increases the ionization level widths calculated from Eq. (3) by ~60%, for all atom-surface separations investigated. It does not, however, change any of our conclusions gleaned from the simple and intuitive expression given in Eq. (3), which therefore is employed in the rest of our analysis.

Figure 2 shows the predicted fraction of Li s-p hybridization (λ_{2p}) as a function of d-band proximity to the Li $2s$ level, for cases where Li is situated 10 a.u. above an on-top site on a variety of fcc(001) metal surfaces. Here we define d-band proximity as the difference between the energy corresponding to the right d-band full width at half maximum (FWHM) and the energy level of the Li $2s$ state. Large, negative d-band proximity values in Fig. 2 correspond to smaller overlap between the Li $2s$ level and the surface d-band. Consequently, as the d-band proximity values become less negative, the Li $2s$ surface d-band overlaps become larger. We observe a nearly perfect correlation (linear regression coefficient of 0.946) between Li s-p hybridization (λ_{2s}) and d-band proximity, suggesting that the hybridization is mediated by the d-band. The data shown in Fig. 2 are generated using a more approximate DFT-PDOS method[20] in order to efficiently survey a large class of transition metal surfaces.

Further evidence of transition metal surface-mediated s-p hybridization is provided by examining the polarization of the electron density for a Li atom outside the metal surface. Figure 3, which displays representative electron density difference ($\Delta\rho$) maps, reveals that electrons in metal surface d-orbitals are involved in the polarization of Li. The quantity $\Delta\rho$ is defined as the difference between density of the interacting system (ρ^{int}) and the sum of the densities of isolated surface (ρ^0_{metal}) and an isolated Li atom (ρ^0_{Li}), $\Delta\rho=\rho^{\text{int}}-\rho^0_{metal}-\rho^0_{\text{Li}}$. Upon analyzing $\Delta\rho$, we find that more than one type of d-orbital contributes. For example, the hybridization is mediated by the Cu $3dz^2$ orbital for Li near Cu(001), whereas the s-p mixing is induced by the Ir $5dx^2-y^2$ orbital for Li near Ir(001). By contrast, while some charge polarization on Li is present near Al and Mg surfaces, it is not enough to produce significant hybridization (as reflected in a low λ_{2p}).

The strength of the mixing is also related to the position and width of the d-band center with respect to the isolated Li $2s$ and $2p$ levels. The Ir and Cu d-band densities of states shown in Fig. 4 indicate that the greater Li level mixing induced by an Ir surface is due to the closer position of the d-band center to the Li $2s$ and $2p$ levels. Late transition

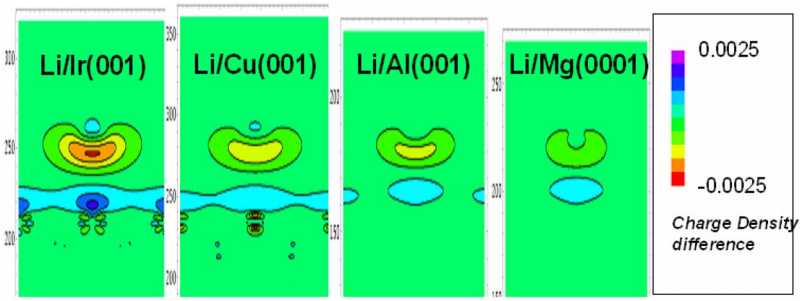

FIG. 3. (Color online) Density difference plots for a Li atom 10 a.u. above top sites on four metal surfaces (Ir(001), Cu(001), Al(001), and Mg(0001)). These absolute differences represent up to ~7.5% changes in density, even at 10 a.u. away from the surface. Greatest polarization of the Li $2s$ occurs above transition metal surfaces and the polarization around the transition metal atoms occurs in patterns characteristic of d-orbitals.

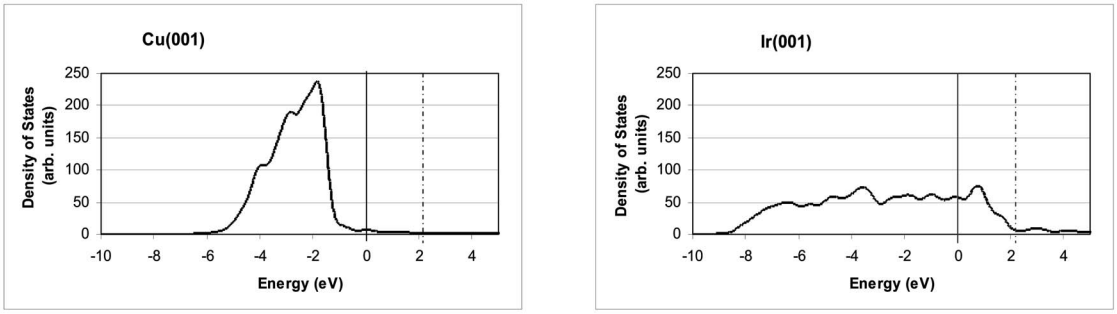

FIG. 4. Metal surface *d*-band DOS for a Li atom 10 a.u. above top sites on (a) Cu(001) and (b) Ir(001) surfaces. Vertical lines at 0 and ~2.1 eV represent the positions of the isolated Li 2*s* and 2*p* levels, respectively. Larger overlap of the *d* band with the Li 2*s* and 2*p* levels correlates with larger mixing.

metals (Groups 8-10) with larger *d*-orbitals and open *d*-shells most effectively induce mixing of the Li levels.

It is conceivable that the intra-atomic hybridization we observe might be due simply to long-range image potential effects induced by the metal surface. We tested this possibility by calculating the intra-atomic hybridization within a jellium model that includes the image potential.[9] This model predicts small λ_{2p} (0.007-0.011) for all metals investigated at an atom-surface separation of 10 a.u., as indicated by the shaded area in Fig. 2. These λ_{2p} values are consistent with our DFT-based predictions for metal surfaces lacking *d*-electrons (e.g., Al and Mg), but not with those for transition metal surfaces: the intra-atomic hybridization predicted by DFT for the latter surfaces are much larger than predicted by the image potential alone. These results further highlight the importance of the *d*-band in mediating the Li *s*-*p* hybridization, since jellium does not account for any effects due to *d*-electrons.

The amount of mixing not only depends on the character of the surface but also on the distance of Li to the surface. The fraction of 2*p* PDOS, λ_{2p} in Eq. (3), varies with Li-surface separation and increases as Li approaches the surface. For small Li-surface separations, the *s*-*p* hybridization is substantial due to the large overlap between the surface *d*-orbitals and the Li orbitals. In general, at each equivalent Li-surface distance, Li *s*-*p* mixing was consistently much greater for transition metal surfaces than for nontransition metal surfaces.

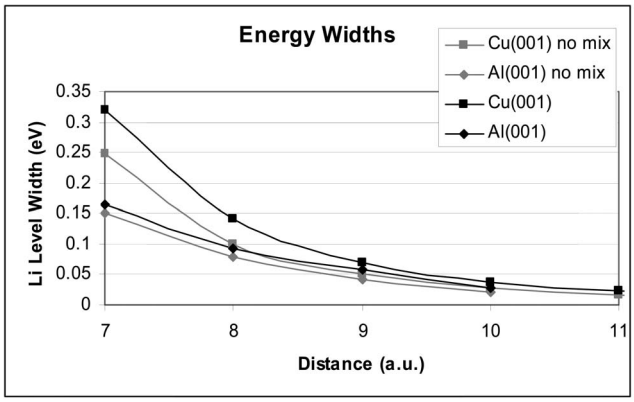

FIG. 5. Broadening of the ionization level of Li as a function of distance from Cu(001) and Al(001), including or neglecting Li 2*s*-2*p* mixing [Eq. (3)]. Although the Li energy level widths for Li near Al(001) are only slightly affected by Li 2*s*-2*p* mixing, the Li widths for Li near Cu(001) are significantly enhanced by accounting for the mixing.

The *s*-*p* hybridization of the energy levels has a noticeable impact on the effective widths of the ionization level of Li near transition metal surfaces. Figure 5 compares the Li widths calculated using Eq. (3) to those obtained neglecting the hybridization, as a function of Li atom-surface separation outside Cu(001) and Al(001). Including Li 2*s*-2*p* mixing has little effect on the widths of Li near Al(001), whereas for Cu and metals with even more *d*-electron character, the effects of Li hybridization are large and crucial for a proper description of the width of the ionization level of Li.

In conclusion, we find strong evidence for a *d*-band mediated intra-atomic hybridization that enhances the mixing of the Li 2*s* and 2*p* states and greatly influences the width of the ionization level of Li outside metal surfaces. These increased widths in turn suggest higher electron tunneling rates outside transition metal surfaces compared to nearly free-electron-like surfaces, consistent with observed trends in chemical reactivity, e.g., transition metals are better catalysts and tend to corrode more easily. A previously developed DFT-based deconvolution technique is used to extract the width of the ionization level. A comparison between transition metal surfaces suggests that larger *d*-band overlap with the Li levels facilitates greater Li 2*s*-2*p* mixing. The amount of level mixing is also reflected in the extent of polarization of the Li electron density. We show that accounting for this mixing is critical for describing the widths of the ionization level of Li. Lastly, validation of the fidelity of our predictions is provided by comparison with the most closely related experimental data available. At a Li-Cu(001) distance of 6 a.u. (close to a chemisorption distance, but large enough where our theory is expected to hold), we predict a lifetime of 8 fs for the ionization level of Li, which compares well with measured lifetimes[23–26] of 6 fs for Cs above Cu(001).

We are grateful to the National Science Foundation (E.A.C.; Grant No. CHE-0201588) and the Robert A. Welch Foundation (P.N.; Grant No. C-1222) for support of this research, and to Accelrys, Inc. for providing the CASTEP software.

[1] J. C. Tully, Annu. Rev. Phys. Chem. **51**, 153 (2000).
[2] B. Hammer and J. K. Norskov, in *Advances in Catalysis*, edited by B. C. Gates and H. Knozinger, Vol. 45 (Academic Press Inc, San Diego, 2000), p. 71.
[3] L. Aballe, A. Barinov, A. Locatelli, S. Heun, and M. Kiskinova, Phys. Rev. Lett. **93**, 196103 (2004).
[4] N. Cabrera and N. F. Mott, Rep. Prog. Phys. **12**, 163 (1948).
[5] H. Petek, H. Nagano, M. J. Weida, and S. Ogawa, J. Phys. Chem. B **105**, 6767 (2001).
[6] J. P. Gauyacq and A. G. Borisov, J. Phys.: Condens. Matter **10**, 6585 (1998).
[7] C. B. Weare and J. A. Yarmoff, Surf. Sci. **348**, 359 (1996).
[8] M. Taylor and P. Nordlander, Phys. Rev. B **64**, 115422 (2001).
[9] K. Niedfeldt, E. A. Carter, and P. Nordlander, J. Chem. Phys. **121**, 3751 (2004).
[10] P. Nordlander and J. C. Tully, Phys. Rev. Lett. **61**, 990 (1988).
[11] D. Teillet-Billy and J. P. Gauyacq, Surf. Sci. **239**, 343 (1990).
[12] P. Kurpick and U. Thumm, Phys. Rev. A **58**, 2174 (1998).
[13] N. Lorente and M. Persson, Faraday Discuss. **117**, 277 (2000).
[14] M. D. Segall, P. J. D. Lindan, M. J. Probert, C. J. Pickard, P. J. Hasnip, S. J. Clark, and M. C. Payne, J. Phys.: Condens. Matter **14**, 2717 (2002).
[15] D. M. Ceperley and B. J. Alder, Phys. Rev. Lett. **45**, 566 (1980).
[16] J. P. Perdew and A. Zunger, Phys. Rev. B **23**, 5048 (1981).
[17] J. P. Perdew, K. Burke, and M. Ernzerhof, Phys. Rev. Lett. **77**, 3865 (1996).
[18] M. C. Payne, M. P. Teter, D. C. Allan, T. A. Arias, and J. D. Joannopoulos, Rev. Mod. Phys. **64**, 1045 (1992).
[19] X. Gonze, G. M. Rignanese, M. Verstraete, J. M. Beuken, Y. Pouillon, R. Caracas, F. Jollet, M. Torrent, G. Zerah, M. Mikami, P. Ghosez, M. Veithen, J. Y. Raty, V. Olevanov, F. Bruneval, L. Reining, R. Godby, G. Onida, D. R. Hamann, and D. C. Allan, Z. Kristallogr. **220**, 558 (2005).
[20] We estimate the overlap integrals appearing in Eq. (1) using the method described in Ref. 27 for the case of ultrasoft wave functions, for the elements shown in Fig. 2. Once the PDOS are calculated in this way, we extract the widths via the deconvolution described previously (Refs. 8 and 9). This approximation produced results that were nearly identical to evaluating Eq. (1) directly, as in Ref. 9.
[21] D. Vanderbilt, Phys. Rev. B **41**, 7892 (1990).
[22] These coefficients turn out to be intuitive: c_{2s} and $-c_{2p}$ from Eq. (2), forming an *sp* hybrid pointing towards the surface.
[23] M. Bauer, S. Pawlik, and M. Aeschlimann, Phys. Rev. B **55**, 10040 (1997).
[24] M. Bauer, S. Pawlik, and M. Aeschlimann, Phys. Rev. B **60**, 5016 (1999).
[25] S. Ogawa, H. Nagano, and H. Petek, Phys. Rev. Lett. **82**, 1931 (1999).
[26] H. Petek, M. J. Weida, H. Nagano, and S. Ogawa, Science **288**, 1402 (2000).
[27] M. D. Segall, R. Shah, C. J. Pickard, and M. C. Payne, Phys. Rev. B **54**, 16317 (1996).